Pergamon

PII: S0038–092X(02)00114–7

Solar Energy Vol. 73, No. 5, pp. 375–384, 2002

0038-092X/03/$ - see front matter

www.elsevier.com/locate/solener

TOWARDS THE DESIGN OF LOW MAINTENANCE SALINITY GRADIENT SOLAR PONDS

M. R. JAEFARZADEH[†,*] and A. AKBARZADEH[**]

*Department of Civil Engineering, Faculty of Engineering, Ferdowsi University of Mashhad, P.O. Box 91775-1111, Mashhad, Iran

**Energy CARE group, Department of Mechanical and Manufacturing Engineering, RMIT University, P.O. Box 71, Bundoora 3083, Melbourne, Australia

Accepted 18 September 2002

Abstract—Applications of simple methods to reduce the maintenance of a small solar pond are discussed in this paper. It was found that floating rings along with continuous surface flushing could effectively control and maintain a relatively thin upper convective layer. A novel system of salt replenishment (a salt charger) is introduced. It is shown that the application of the proposed system is capable of controlling the position of the lower interface. Criteria governing the design of a salt-charger for a salinity-gradient solar pond are developed theoretically and verified experimentally. The design procedures are presented. Experiences relating to the utilization of brine shrimps to improve the transparency of the pond are described.

1. INTRODUCTION

Salinity-gradient solar ponds have been accepted as simple and reliable sources of solar energy for many years. Since the operation of early ponds (Tabor and Matz, 1965), considerable theoretical and experimental work has been carried out to understand the physics of the solar pond (Tabor and Weinberger, 1980).

Practically, the main problems encountered in the maintenance of salinity-gradient solar ponds are limiting the thickness of the upper convective zone (UCZ), controlling the position of the interface between the gradient layer or non-convective zone (NCZ) and the lower convective zone (LCZ), and retaining an acceptable level of water clarity. Tackling these problems in order to ensure the hydrodynamic stability of the pond, as well as a reasonable thermal efficiency, generally requires a substantial amount of effort.

This paper attempts some proposals for reducing the maintenance of solar ponds as much as possible, and their application to a small-scale solar pond.

2. DESCRIPTION OF THE SOLAR POND

An experimental salinity-gradient solar pond was constructed in the Renewable Energy Laboratory of the Department of Mechanical and Manufacturing Engineering, RMIT, in Melbourne (37°49′ S, 144°58′ E). The pond was circular in plan with a diameter of 8 m and a total area of 50 m^2. Its wall and base were made up of reinforced concrete with a thickness of 0.2 m. The surface of the concrete was coated with a 1-mm layer of epoxy resin to protect the concrete against corrosion and possible chemical reactions between salt and concrete. The level of water in the pond was fixed at 2.26 m above the bed using an overflow system, and the bed level was 1.36 m below the ground level as shown in Fig. 1a. Fresh water continuously flowed from a mains tap to flush the surface and compensate for evaporation. Typically, the rate of flushing was about twice the evaporation rate. Floating rings were distributed over the surface of the pond to reduce the surface mixing caused by wind-driven currents. Each ring was made from a high-density polyethylene (HDPE) strip with 35 mm width and 1.5 mm thickness. The ends of the strip were fastened together to form a circle with a diameter of 0.6 m. The density of the HDPE was just less than the density of water (940 kg/m^3). Therefore the top edge of the rings protruded slightly above the surface of the pond. The rings were connected to each other by plastic strings to prevent overlapping. The floating rings suppress wave action by dividing up the surface area of the pond into small isolated cells to reduce the fetch length, which in turn limits the wave lengths and hence amplitudes of the waves (Akbarzadeh *et al*., 1983).

A salt charger was employed to replenish the

[†]Author to whom correspondence should be addressed. Fax: +98-511-8436433; e-mail: jafarzad@ferdowsi.um.ac.ir

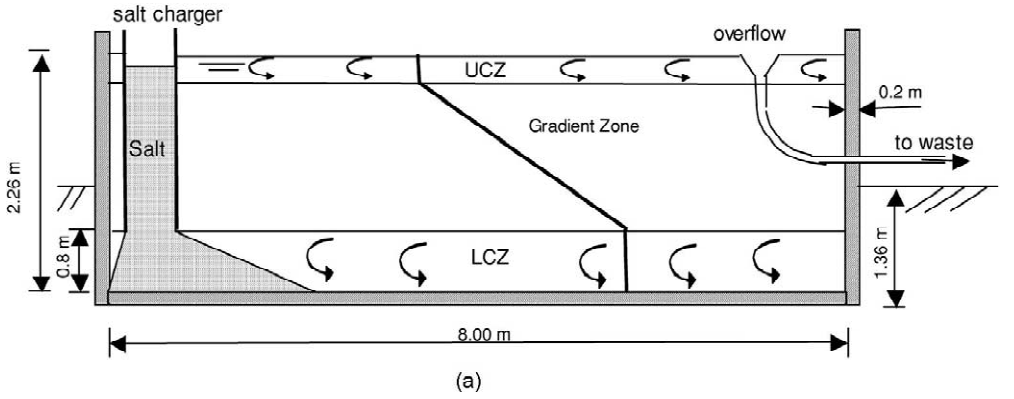

(a)

(b)

Fig. 1. (a) Schematic view of the pond with three zones, salt charger and surface washing system. (b) RMIT solar pond at Bundoora: the presence of the window (Eastward) facilitated the visual observation of water clarity at different depths. Floating rings and salt charger are clearly shown in the picture.

salt (NaCl) in the pond. The charger was made from a polyethylene cylinder with a diameter of 0.61 m fixed to the wall of the pond. The bottom of the cylinder, which was open, was located 0.80 m above the bottom of the pond. The cylinder was filled with salt up to the surface of the pond. Salt coming out of the bottom of the cylinder produced a salt pile in the shape of a semi-cone round the charger. A sketch of a cross section of the pond with three zones, surface washing, outlet system and salt charger is shown in Fig. 1a. Fig. 1b shows a photograph of the experimental solar pond. The fact that the pond was partly above the ground proved to be of great value. This enabled the operation of the overflow system and made maintenance of the water level in the pond very easy and basically without the need of any attention. Also it facilitated visual inspection of the pond. The concrete wall was also used for mounting equipment such as the salt charger, a scanning mechanism to measure temperature and salinity, as well as a diffuser system needed to set up the gradient. A 0.4 m wide, 1.5 m tall glass window (10 mm thickness), installed on

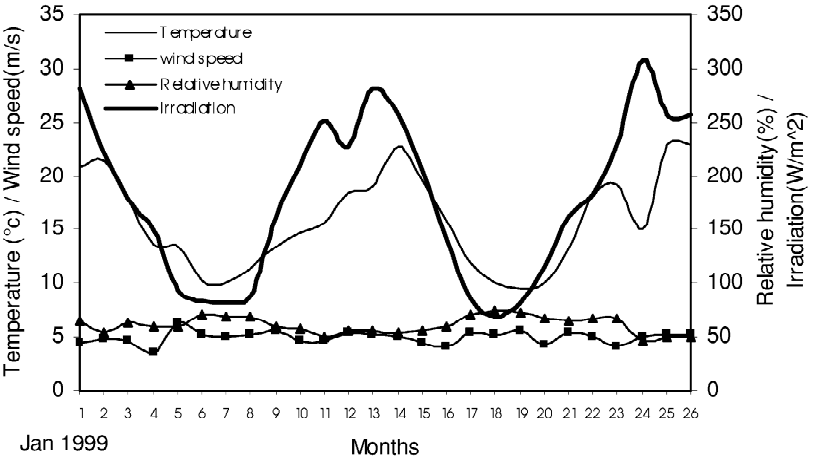

Fig. 2. Monthly averages of climatological parameters in a site near to the solar pond.

the western side of the pond, proved very useful in observing clarity of the interior of the pond and also for monitoring the movements of brine shrimps at different levels in the pond.

3. PERFORMANCE OF THE POND

The solar pond at RMIT's Bundoora campus has been continuously running since 18 March 1999. Fig. 2 shows the climatological situation of a site near to the pond since January 1999. Fig. 3 shows the variation of the temperature of the LCZ and UCZ since the pond started operating. During the first year, the pond was warming up and the temperature of the LCZ increased uniformly since it began operation until it reached a maximum of 55°C in January 2000. It remained above 50°C for about 5 months and then declined. The minimum temperature of about 27°C occurred in July 2000. The temperature of the UCZ changed from a minimum of 10°C in July to a maximum of 27°C in January, varying with the ambient temperature.

In Fig. 4 the densities of the LCZ and UCZ are plotted versus time. Both densities remained fairly constant. The density of the UCZ was close to that of pure water because of continuous flushing, and the density of the LCZ was close to saturated brine because of the presence of the pile of salt in the LCZ, as shown in Fig. 1a.

In Fig. 5, the water level position and variation of the positions of the upper and lower interfaces are plotted against time. As mentioned, the surface of the pond was fixed at 2.26 m above the bottom of the pond by continuous flushing and the overflow system. It can be seen that the thickness of the LCZ remained constant (0.8 m). The thick-

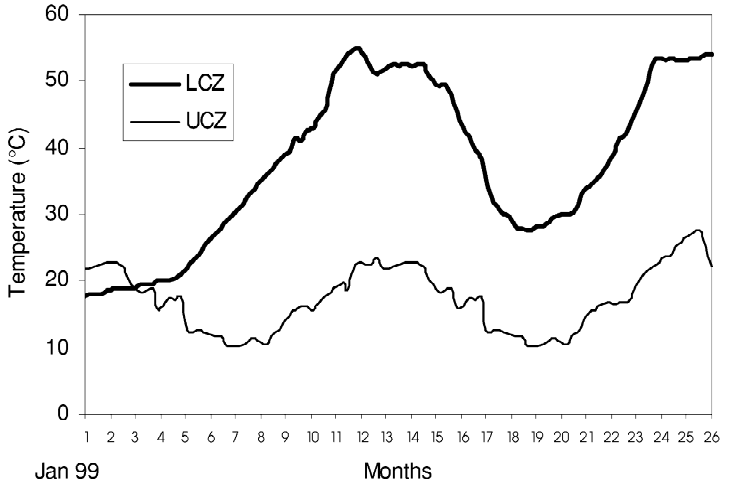

Fig. 3. Temperature variations in the lower and upper convective zones.

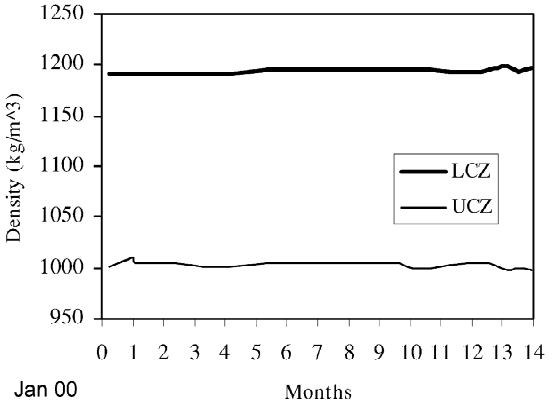

Fig. 4. Variations of the density of the upper and lower convective layers.

ness of the UCZ was slightly variable, but did not exceed 0.25 m. Therefore, the thickness of the gradient layer was fairly constant at about 1.2 m.

In Fig. 6a some typical salinity profiles at different times are presented. Some local convective layers are evident in the gradient zone. However, after a while, these layers disappeared because of high brine concentration of the LCZ, resulting in a strong gradient.

In Fig. 6b temperature profiles are plotted for the same period as the salinity profiles. The existence of some small local instabilities may also be deduced from these profiles. It has been shown that the sidewalls can possibly generate such convective layers (Akbarzadeh and Manins, 1988; Akbarzadeh, 1989).

In Fig. 7 variations of temperature at various depths in the ground below the centre of the pond were plotted for 15 days. It is seen that daily fluctuation of temperature was profound even at 1 m below the base level. In fact the concrete base was not a good insulator and it was estimated that at least 35% of the total energy that reached the

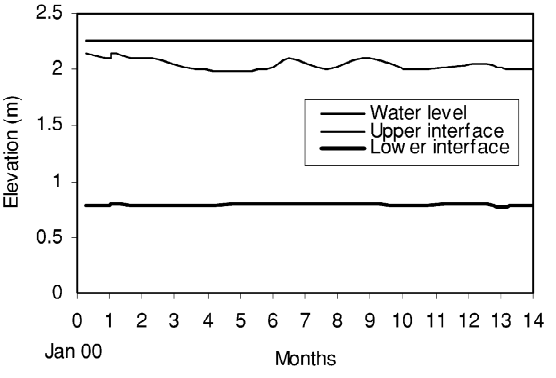

Fig. 5. Variations of the position of the water level, upper and lower interfaces.

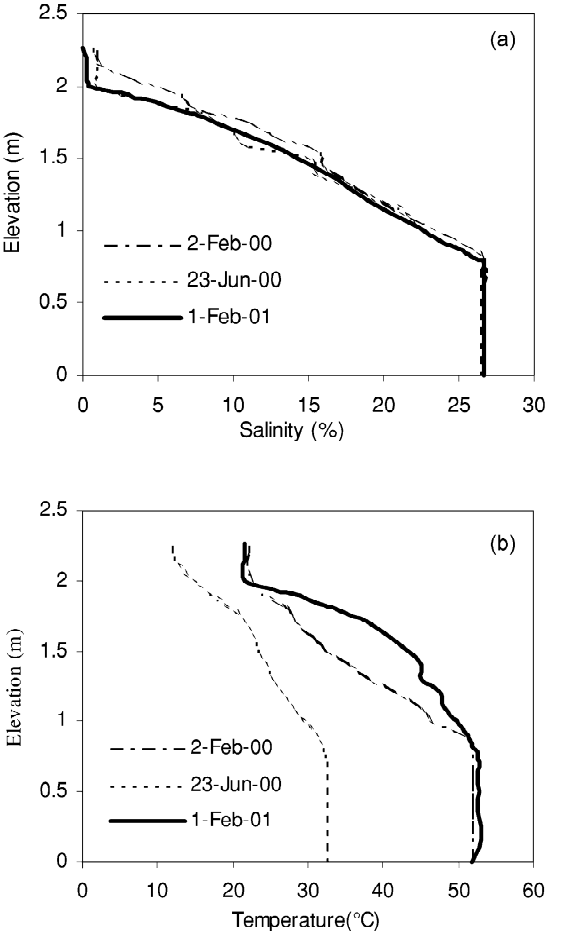

Fig. 6. (a) Salinity profiles. (b) Temperature profiles.

LCZ was lost to the ground. This loss was responsible for the relatively low temperature of the LCZ in spite of a deep gradient layer. Another reason can be attributed to the shading effect of the walls (due to high latitude) that reduced the effective area of the pond considerably.

4. MAINTENANCE OF THE UPPER AND LOWER INTERFACES

Located in an open space area where uncertainties in both environment and weather are prevalent, a solar pond can generate instabilities and malfunctioning if maintenance is not carefully carried out. A major part of the maintenance of a solar pond consists of procedures to control thickness and salinities of the UCZ and LCZ for an efficient performance.

The thickness of the UCZ has a pronounced effect on the efficiency of the solar pond (Wang and Akbarzadeh, 1983). Ideally, this layer needs to be as thin as possible. In a study with a small 4 m^2 solar pond with the surface unprotected, the

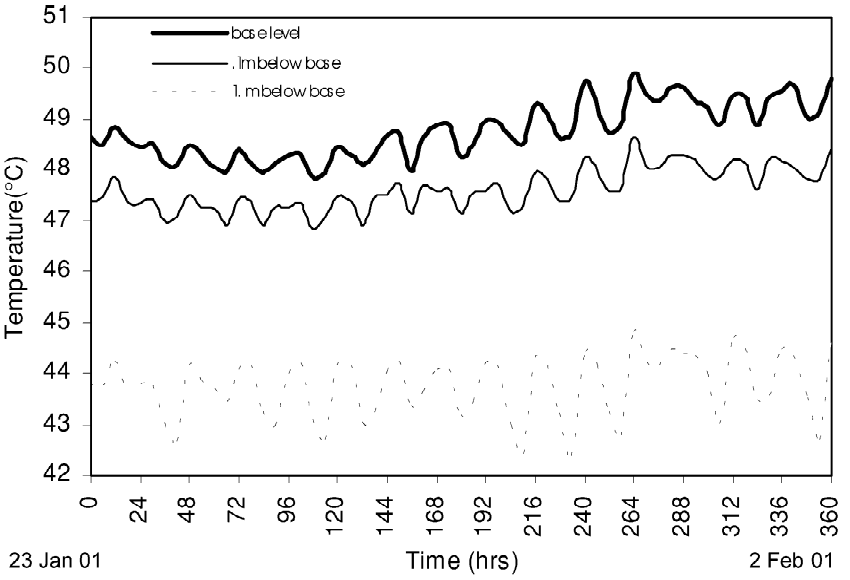

Fig. 7. Variations of temperatures at various depths in the ground below the center of the pond.

depth of the upper zone increased to 0.30 m (Jaefarzadeh, 2000). However, in spite of the application of some surface protection measures in the form of nets, the thickness of the UCZ in most experimental solar ponds has been in excess of 0.5 m (Hull *et al*., 1989). In the present study it was observed that a combination of continuous surface flushing and floating rings were successful in reducing and maintaining the thickness of the UCZ to lower than 0.25 m as seen in Fig. 5.

The design criteria for the rings and the determination of their respective diameter and height have been discussed in detail (Akbarzadeh *et al*., 1983). The favorable experimental results obtained in the present pond that was protected with floating rings supports the conclusion that these rings are effective.

The salt charger also satisfactorily maintained the LCZ. Similar observations in controlling the position of the lower interface have also been reported by Newell *et al*. (1990) at the University of Illinois's Solar Pond and Hull *et al*. (1986) at the Argonne National Laboratory Salt Gradient Solar Pond. At the start of the pond operation, the density of the LCZ was very near to the density of saturated brine (NaCl). However, there was a continuous diffusion of salt to the upper zones. The salt in the semi-cone around the charger, gradually dissolved into the LCZ to compensate for the upward diffusion and prevent the reduction of its salinity. The pile of salt stored in the charger provided the required deficit to keep the lower convective zone in close saturation. Normally a bag of 25 kg salt was enough for 1 week of pond operation (corresponding to an upward diffusion rate of $70\,g/m^2$ day). This was about 10% more than the mass diffusion obtained theoretically. Possibly, local convective layers in the gradient zone combined with eddies generated either by surface driven currents or by brine shrimps swimming up and down were responsible for the enhancement of salt transport. However, as reported previously (Srinivasan, 1990; Tabor, 1981), this amount of salt consumption is quite reasonable due to the relatively thick gradient layer. In the following section the design of a salt charger is investigated theoretically and experimentally.

5. DESIGN OF SALT CHARGER

The design of a salt charger aims at finding its dimensions and it depends on several parameters such as pond surface area, salt consumption rate, and thickness of the lower convective zone. In order to investigate the design criteria, a theoretical model of a salt charger in a solar pond was developed. The validity of the model was later tested experimentally.

5.1. Theoretical considerations for salt dissolving by natural convection

For the sake of simplicity, the problem is assumed to be two-dimensional in which a layer of fresh water overlays a saline layer in a rectangular container, as depicted in Fig. 8, where a slope was formed by salt coming out of a salt charger. Consider the control volume of ABCD as

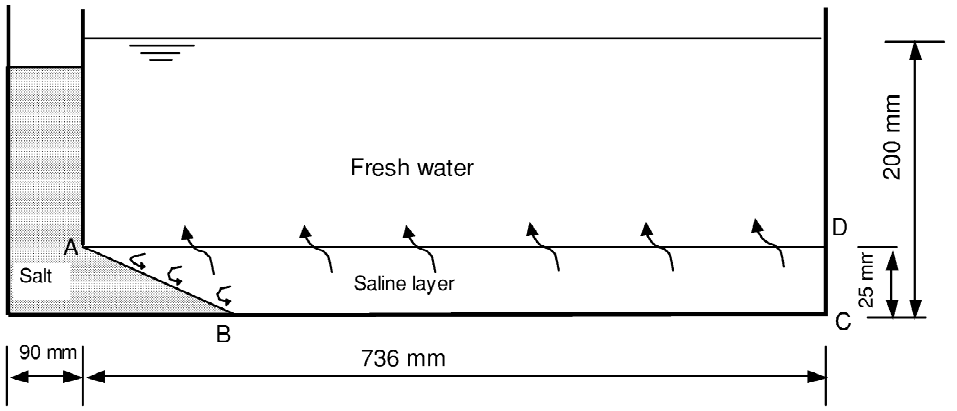

Fig. 8. Schematic of the experimental laboratory tank. It was made of 6-mm-thick clean plastic sheets. The width of the tank was 99 mm.

shown in the figure. It may be assumed to be a cross-section of a saline layer. The salt resting at AB produces a flow of brine in a thin boundary layer over the slope. The saline flow mixes into the control volume and diffuses out of it through the upper interface AD, into the fresh water layer.

In analogy with free convection heat transfer, we can write the following equation on the boundary layer AB

$$Q_i = hA_s(C_s - C_o) \tag{1}$$

where Q_i is the input mass transfer rate in kg/s, h is the convection mass transfer coefficient in m/s, A_s is the area of the slope in m^2, C_s is the concentration of brine at the slope in kg/m^3 and C_o is the average of concentration in the saline layer. It may be assumed that the brine at the boundary layer over the slope is fully saturated.

The diffusion of salt at the interface AD can be written as:

$$Q_o = DA_p \frac{\partial C}{\partial Z} \tag{2}$$

where Q_o is the rate of mass diffusion (kg/s) through the interface, A_p is the area of the interface (m^2), and D is the coefficient of diffusivity of salt in m^2/s. Z is the vertical axis and is assumed positive downward.

Assuming a quasi steady state situation we can write

$$Q_i = Q_o. \tag{3}$$

In other words the rate of mass dissolving into the saline layer is equal to the rate of mass diffusing out of the saline layer and into the fresh water region.

As a result, the coefficient of convective mass transfer can be obtained:

$$h = D\frac{A_p}{A_s}\frac{\partial C}{\partial Z}\frac{1}{C_s - C_o}. \tag{4}$$

In analogy with the classical theory of convection heat transfer (Holman, 1986), for the free laminar convection of mass over a vertical plate at a distance of x along the plate, we can write

$$Sh_x = 0.508\, Sc^{1/2}(0.952 + Sc)^{-1/4} Gr_x^{1/4} \tag{5}$$

where Sh_x is the Sherwood number, a counterpart for the Nusselt number, and at point x (m) along the plate is defined by $Sh_x = hx/D$, Sc is the Schmidt number, a counterpart of the Prandtl number and is defined by $Sc = \nu/D$ in which ν is the kinematic viscosity of saline in m^2/s. Gr_x is the Grashof number defined by

$$Gr_x = \frac{g\beta(C_s - C_o)x^3}{\nu^2} \tag{6}$$

in which $\beta = 1/\rho\ \partial\rho/\partial C$ is the expansion coefficient of density due to concentration in m^3/kg. Here ρ is the density of the liquid in kg/m^3.

For the case of a finite plate with length L, the average mass transfer coefficient is given by

$$\bar{h} = \frac{1}{L}\int_0^L h_x\, dx. \tag{7}$$

Taking an average for h_x in Eq. (7), we can write

$$\bar{h} = \frac{4}{3} h_{x=L}. \tag{8}$$

For the laminar flow, we should have $Ra_x = Gr_x.Sc \leq 10^9$, where Ra_x is the Rayleigh number at x.

Based on empirical measurements Churchill and Chu (1975) gave the following correlations:

$$\overline{Sh} = 0.68 + \frac{0.67\, Ra_L^{1/4}}{\left[1 + \left(\frac{0.492}{Sc}\right)^{9/16}\right]^{4/9}} \qquad Ra_L \le 10^9 \tag{9}$$

and

$$\overline{Sh} = \left\{0.825 + \frac{0.387 Ra_L^{1/6}}{\left[1 + \left(\frac{0.492}{Sc}\right)^{9/16}\right]^{8/27}}\right\}^2$$

$$0.1 \le Ra_L \le 10^{12} \tag{10}$$

where the first equation gives a better accuracy for laminar flow and the second one is applied for a full range of Ra_L.

For an inclined plate it is recommended to replace g by $g \cos(\theta)$ in computing the plate Rayleigh number, where θ is the angle of slope between the plate and vertical direction.

5.2. Experimental observation

A series of experiments was conducted in the laboratory simulating a cold pond. The experimental container, rectangular in plan with a width of 99 mm, was made of Plexiglas sheets with a thickness of 6 mm. A sheet of Plexiglas separated the container into two compartments. The first part simulated a salt charger and the second part simulated a pond, Fig. 8. The bottom of the sheet was 25 mm above the bed of the container. At the start of the experiment, the container was filled with pure water to a depth of 200 mm and the charger was filled with ordinary granular table salt. A block closed the bottom opening of the charger. After removal of the block, the granular salt came out of the opening and a slope was formed. The angle of slope was ~70° from the vertical direction. Then a free convective boundary layer caused by saline flow was produced over the slope. A shadowgraph was used to observe the flow pattern (Akbarzadeh and Manins, 1988). The flow was laminar at the upper part of the slope, where the boundary layer was developed. However, at some distance along the slope, turbulent eddies were formed and the transition to a turbulent boundary layer began. The flow was quite turbulent towards the end of the slope. At the bottom of the container a saline front ran over the bed. Later on, the continuous flow of dissolved salt formed a nearly saturated saline layer. A very slow circulation took place in this layer, where the currents were far from the slope at the bed and towards the slope at the interface with fresh water above it. Gradually, the depth of the saline layer increased and at the same time mass diffusion caused migration of salt to the upper layer of fresh water. In Fig. 9, by taking samples at points with 5-mm intervals, salinity profiles in depth were plotted at various times. The saline layer that built up itself very quickly in a few hours started diffusing to the upper fresh layer. It is also interesting that at any time after the rise of interface to the top of the slope, the salinity profile was fairly uniform and near to saturation over the thickness of the saline layer. However, the salinity concentration gradient $\partial C/\partial Z$ at the interface decreased with time as deduced from Fig. 9. As a result, the average concentration C_o was changed slightly. Based on our measurements we assumed $C_s = 313.3\ \mathrm{kg/m^3}$ at 20°C.

The coefficient of mass transfer, h, based on experimental observations and calculated from Eq. (4) at various times is shown in Fig. 10. The same coefficient obtained from laminar flow theory (Eq. (5)) and from empirical correlations is also shown in the figure. It is seen that Eq. (9) is

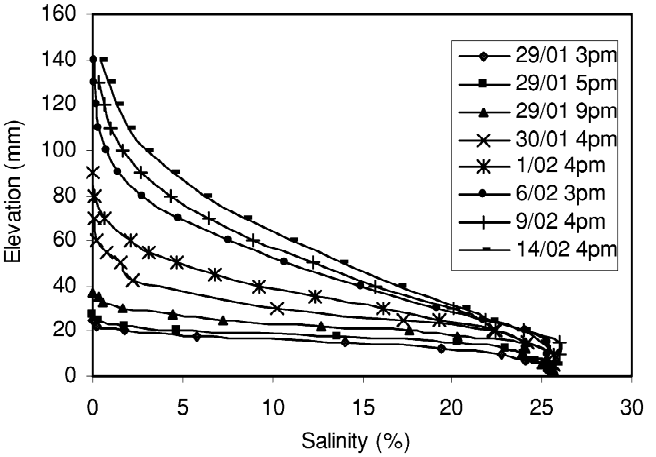

Fig. 9. Time development of salinity profile.

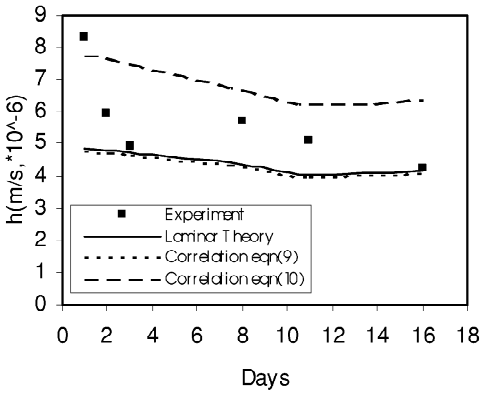

Fig. 10. The coefficient of convective mass transfer.

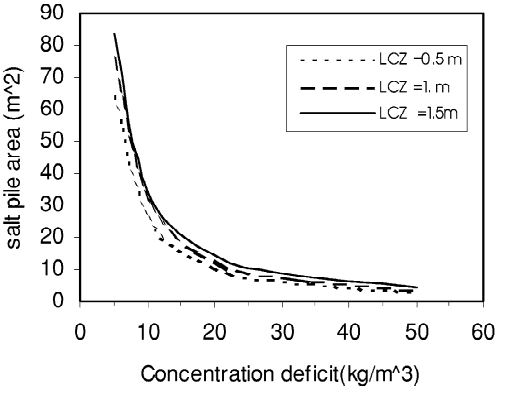

Fig. 11. Required salt pile area design curves for a 1000 m^2 salt gradient solar pond.

nearly coincident with laminar flow theory. However, Eq. (10) for a wider range of *Ra* gives higher values for *h* as expected. Apart from the initial experimental data at the transient stage (first day), the latest values could be placed in a band between the curves. They approached the laminar flow curve gradually as time passed. The average Rayleigh number in these experiments was about 5×10^9.

5.3. Design procedure for the salt charger

The following algorithm can be used for the design of a salt charger in a solar pond.

1. Assume a concentration deficit value for $\Delta C = (C_s - C_o)$. In our experiments this value was in the range of 5 to 30 kg/m^3.
2. Assuming a certain height for the salt pile and a certain slope, calculate $\bar{h}$ from laminar flow theory (Eq. (5)) or correlation equations (Eqs. (9) or (10)), conveniently. From Fig. 10, it can be deduced that laminar flow theory will give a conservative value for $\bar{h}$.
3. Calculate the flux of mass transfer (salt) over the salt pile, $q = \bar{h}(C_s - C_o)$.
4. Estimate a suitable value for the rate of upward salt transfer per unit area of the pond based on the salinity difference of the LCZ and UCZ, gradient layer thickness and salt diffusivity. Then calculate the total rate of mass transfer, $\dot{m}$ (kg/s), for the entire pond.
5. Calculate the required area A_s, of the salt pile from

$$A_s = \frac{\dot{m}}{q}. \tag{11}$$

In Fig. 11 following the above procedure, curves showing the required salt pile area A_s versus concentration deficit ΔC are drawn for several thicknesses of LCZ. Here the pond area is assumed to be 1000 m^2 and salt transfer rate per unit area is assumed to be 70 g/m^2 day. Salt is assumed to be NaCl with a diffusivity of 3×10^{-9} (m^2/s) which is at 60°C.

It is seen that the thickness of the LCZ is not so much effective on A_s. On the other hand, increase in ΔC will decrease A_s considerably. Notably, having a small value of ΔC that means being close to saturated concentration, maintains a strong gradient layer for a pond, which is important from the stability point of view. Therefore it can be deduced that assuming $\Delta C \approx 20$ kg/m^3, may optimise A_s for different thicknesses of LCZ. This point corresponds to a salt pile area of 10 m^2. Considering the assumed area of 1000 m^2, this corresponds to 1% of solar pond area. Fig. 11 can be used as a design guide for any other pond area and mass transfer rate per unit area provided that the ordinate is proportionally corrected.

6. CLARITY OF THE POND

Maintaining the clarity of a solar pond usually concerns the designer from the outset. Plant life is an agent that could be responsible for the reduction in clarity. With increasing salinity, only specific microorganisms, including a few species of algae (e.g. Dunaliella) could survive in a solar pond (Hull *et al.*, 1989).

While chemical methods (e.g. chlorination or acidification) are very common for controlling algal growth, use of natural clarification techniques seems to be promising. The brine shrimp species *Artemia salina* is found in saltworks evaporation ponds (Tackaert and Sorgeloos, 1993). They can also be utilized in the upper half depth of solar ponds for improving transparency. The shrimps swim in the pond and feed on algal

populations and detritus, which are a major source of turbidity. The material ingested by the shrimp is excreted as dense fecal pellets, which sink down to the bottom of the pond (Hull, 1989). The growth and survival of the brine shrimp are greatly influenced by temperature and salinity. Although adults can tolerate brief exposures to temperatures as extreme as −18 to 40°C, the common range of preference is 19 to 25°C. Considering salinity, the upper limit of survival is about 200–250 ppt, however, the range of preference is 35–110 ppt, in which mortality is less than 10%. Above 30°C temperatures and under 20 ppt salinity soon become lethal for most strains. The pH tolerance for *Artemia* ranges from 6.5 to 8. With regard to oxygen, only concentrations of less than 2 ppm can limit the production of biomass. For optimal production, however, greater concentrations of O_2 have been suggested (Lavens and Sorgeloos, 1991).

The application of brine shrimps (*Artemia franciscana*) in the RMIT solar pond at Bundoora improved the clarity so much that the bottom of the pond could be seen easily. The brine shrimps used to swim in the upper 1 m of the pond and occasionally they would dive down to the lower interface as was observed from the side window. In addition to visual observations of the pond, the turbidity of the water was also measured by taking samples from different depths and using a conventional turbidity meter. Measurements indicated that the turbidity in the upper convective zone and the gradient zone was generally less than 1 NTU. In the lower convective zone the water seemed to have higher turbidity. This was not considered a source of concern as absorption of light in that region which acts as a thermal storage is in fact desirable.

No attempt has been made yet to quantify the population of brine shrimps and to measure their concentration. However, it was noticed that their population decreased substantially in the colder parts of the year and at some stage it was thought that they completely vanished. However, by the emergence of spring, brine shrimps became visible again, at mid summer their population was back to the level observed the year before and they thrived in the pond for quite some time with a minimum of supervision.

7. CONCLUSIONS

The small thickness of the upper convective zone of the RMIT experimental solar pond is attributed to the combined effect of continuous surface flushing achieved by the proposed gravity operating overflow system, and also to floating rings which reduce the fetch length of the surface waves caused by wind. A floating-ring wave suppression system along with surface washing can thus offer a viable and maintenance-free method of controlling the thickness of upper convective zone.

The proposed salt charger has also proven to be able to fix the position of the lower interface. Through this method, salt can be replenished in salinity-gradient solar ponds. Design criteria for such salt chargers are also provided. It is seen that the required surface area of the salt pile does not strongly depend on the thickness of LCZ and it mainly depends on the overall rate of salt transport in the pond, as well as the desired level of salt concentration at the bottom of the pond. Based on the developed design guidelines an area of 1% of the total solar pond area would offer sufficient surface area for the salt pile to compensate for upward diffusion of salt in most solar ponds

Brine shrimps can play a role in maintaining a reasonable clarity in salt gradient solar ponds. During the period of operation of the RMIT solar pond, no maintenance was needed for the clarity. However, care needs to be taken to avoid the pond becoming contaminated with chemicals that are harmful to brine shrimps.

Acknowledgements—The financial supports of Ferdowsi University of Mashhad and the Australian Greenhouse Office, during the preparation of this work, are kindly acknowledged. It is also a pleasure to thank Mr. Oanca for his cooperation in salinity and temperature measurements. Special thanks are offered to Mr. John Andrews for his useful comments towards the improvement of the manuscript.

REFERENCES

Akbarzadeh A. and Manins P. (1988) Convective layers generated by sidewalls in solar ponds. *Solar Energy* **41**, 521–529.

Akbarzadeh A. (1989) Convective layers generated by sidewalls in solar ponds: observations. *Solar Energy* **43**(1), 17–23.

Akbarzadeh A., Mac Donald R. W. G. and Wang Y. F. (1983) Reduction of surface mixing in solar ponds by floating rings. *Solar Energy* **31**(4), 377–380.

Churchill S. W. and Chu H. H. S. (1975) Correlating equations for laminar and turbulent free convection from a vertical plate. *Int. J. Heat Mass Transfer*. **18**, 1323.

Holman J. P. (1986). *Heat Transfer*, McGraw-Hill.

Hull J. R. (1989) Maintenance of brine transparency in salinity gradient solar ponds. In *ASME, Solar Energy Division Conference*, San Diego, CA, April.

Hull J., Nielsen C. E. and Golding P. (1989). *Salinity Gradient Solar Ponds*, CRC Press, Boca Raton, FL.

Hull J. R., Scranton A. B., Mehta J. M., Cho S. H. and Kasza K. E. (1986). *Heat Extraction from the ANL Research Salt Gradient Solar Pond, Report No. ANL-86-17*, Argonne National Laboratory, Argonne, IL.

Jaefarzadeh M. R. (2000) On the performance of a salinity gradient solar pond. *Appl. Thermal Eng.* **20**, 243–252.

Lavens P. and Sorgeloos P. (1991) Production of *Artemia* in culture tanks. In *Artemia Biology*, Browne Sorgeloos R. A. and Tortman C. N. A. (Eds.), CRC Press, Boca Raton, FL.

Newell T. A., Cowie R. G., Upper J. M., Smith M. K. and Cler G. L. (1990) Construction and operation activities at the University of Illinois salt gradient solar pond. *Solar Energy* **45**(4), 231–239.

Srinivasan J. (1990) Performance of a small solar pond in tropics. *Solar Energy* **45**(4), 221–230.

Tabor H. and Weinberger Z. (1980) Nonconvecting solar ponds. In *Solar Energy Handbook*, Kreider J. F. and Kreith F. (Eds.), p. 10, McGraw-Hill, New York.

Tabor H. and Matz R. (1965) Solar pond project. *Solar Energy* **9**, 177.

Tabor H. (1981) Solar ponds. *Solar Energy* **27**(3), 181–194.

Tackaert W. and Sorgeloos P. (1993) The use of brine shrimp, *Artemia* in biological management of solar saltworks. In Seventh Symposium on Salt, Vol. I, pp. 617–622, Elsevier Science, Amsterdam.

Wang Y. F. and Akbarzadeh A. (1983) A parametric study on solar ponds. *Solar Energy* **30**(6), 555–562.